Science of the Total Environment 650 (2019) 2085–2094

Contents lists available at ScienceDirect

Science of the Total Environment

journal homepage: www.elsevier.com/locate/scitotenv

Ecotoxicity of the lipid-lowering drug bezafibrate on the bioenergetics and lipid metabolism of the diatom *Phaeodactylum tricornutum*

Bernardo Duarte [a,*], Diogo Prata [b], Ana Rita Matos [b], Maria Teresa Cabrita [c,1], Isabel Caçador [a], João Carlos Marques [d], Henrique N. Cabral [a,e], Patrick Reis-Santos [a,f], Vanessa F. Fonseca [a]

[a] MARE - Marine and Environmental Sciences Centre, Faculdade de Ciências da Universidade de Lisboa, Campo Grande, 1749-016 Lisbon, Portugal
[b] BioISI - Biosystems and Integrative Sciences Institute, Plant Functional Genomics Group, Departamento de Biologia Vegetal, Faculdade de Ciências da Universidade de Lisboa, Campo Grande, 1749-016 Lisboa, Portugal
[c] Instituto do Mar e da Atmosfera (IPMA), Rua Alfredo Magalhães Ramalho, 6, 1495-006, Algés, Lisboa, Portugal
[d] MARE - Marine and Environmental Sciences Centre, c/o Department of Zoology, Faculty of Sciences and Technology, University of Coimbra, 3000 Coimbra, Portugal
[e] Irstea, UR EABX (Ecosystèmes Aquatiques et Changements Globaux), 50 avenue de Verdun, 33610 Cestas, France
[f] Southern Seas Ecology Laboratories, School of Biological Sciences, The University of Adelaide, SA 5005, Australia

HIGHLIGHTS

- High Bezafibrate concentrations increased cell density, promoted by a shift from autotrophic to mixotrophic metabolism.
- Bezafibrate can be used by diatoms as carbon source, along with light-generated redox potential.
- The concentrations of plastidial marker fatty acids showed negative correlations with Bezafibrate exposure.
- This metabolic shift derived from bezafibrate exposure may reduce O_2 generation and CO_2 fixation.

GRAPHICAL ABSTRACT

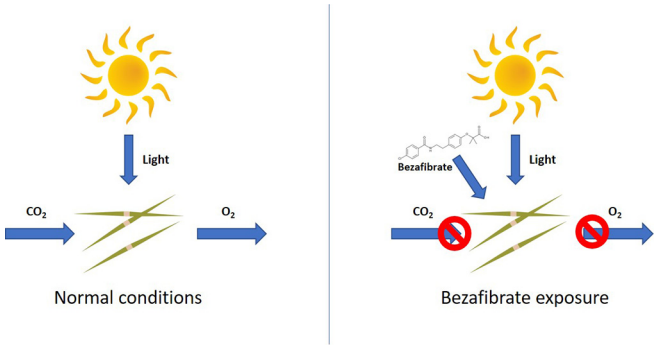

ARTICLE INFO

Article history:
Received 8 May 2018
Received in revised form 24 September 2018
Accepted 28 September 2018
Available online 01 October 2018

Editor: Henner Hollert

Keywords:
Fibrates
Pharmaceuticals
Marine primary producer
Photochemistry
Fatty acids

ABSTRACT

Pharmaceutical residues impose a new and emerging threat to the marine environment and its biota. In most countries, ecotoxicity tests are not required for all pharmaceutical residues classes and, even when mandatory, these tests are not performed using marine primary producers such as diatoms. These microalgae are among the most abundant class of primary producers in the marine realm and key players in the marine trophic web. Blood-lipid-lowering agents such as bezafibrate and its derivatives are among the most prescribed drugs and most frequently found human pharmaceuticals in aquatic environments. The present study aims to investigate the bezafibrate ecotoxicity and its effects on primary productivity and lipid metabolism, at environmentally relevant concentrations, using the model diatom *Phaeodactylum tricornutum*. Under controlled conditions, diatom cultures were exposed to bezafibrate at 0, 3, 6, 30 and 60 μg L^{-1}, representing concentrations that can be found in the vicinity of discharges of wastewater treatment plants. High bezafibrate concentrations increased cell density and are suggested to promote a shift from autotrophic to mixotrophic metabolism, with diatoms using light energy generated redox potential to breakdown bezafibrate as carbon source. This was supported by an evident increase in cell density coupled with an impairment of the thylakoid electron transport and consequent photosynthetic activity reduction. In agreement, the concentrations of plastidial marker fatty acids showed

* Corresponding author.
E-mail address: baduarte@fc.ul.pt (B. Duarte).
[1] Present affiliation: Centro de Estudos Geográficos (CEG), Instituto de Geografia e Ordenamento do Território (IGOT), University of Lisbon, Rua Branca Edmée Marques, 1600-276 Lisbon, Portugal).

https://doi.org/10.1016/j.scitotenv.2018.09.354

negative correlations and Canonical Analysis of Principal coordinates of the relative abundances of fatty acid and photochemical data allowed the separation of controls and cells exposed to bezafibrate with high classification efficiency, namely for photochemical traits, suggesting their validity as suitable biomarkers of bezafibrate exposure. Further evaluations of the occurrence of a metabolic shift in diatoms due to exposure to bezafibrate is paramount, as ultimately it may reduce O_2 generation and CO_2 fixation in aquatic ecosystems with ensuing consequences for neighboring heterotrophic organisms.

1. Introduction

Over the last decades significant attention has been directed to the effects of the so-called "classical contaminants" (e.g. trace metals) in marine biota and their metabolism (Thomaidis et al., 2012). Recently, there are suites of contaminants of emerging concern that present new challenges and risks to natural ecosystems, as the result of the continuous uncontrolled development of multiple human activities (Gavrilescu et al., 2015). Emerging pollutants (EPs) include a wide range of man-made chemicals used daily worldwide (such as pesticides, cosmetics, personal and household care products, pharmaceuticals) (Thomaidis et al., 2012). Between 2002 and 2011, over 50% of the total production of chemicals comprised environmentally harmful compounds, of which over 70% have significant environmental impact (EUROSTAT, 2017). The continued increase in the chemical synthesis industry, reflects the speed of synthetic chemical innovation (CAS, 2011), with several of these novel substances rising concerns regarding their ecotoxicological effects and how to assess them efficiently.

In comparison with classical contaminants, and in large part due to the analytical procedures required, only more recently has there been a commitment to study the release and effects of pharmaceuticals from sewage and other land-base sources into coastal and marine environments (Gaw et al., 2014), in particular near the outfalls of treated and untreated sewage outfalls where pharmaceutical residues can appear in particularly high concentrations (namely at $\mu g/L^{-1}$ concentrations) (Reis-Santos et al., 2018; Thomas and Hilton, 2004). Blood-lipid-lowering agents such as bezafibrate and the metabolization production of different fibrates, are among the most commonly prescribed drugs and also among the most frequently detected human pharmaceuticals in the aquatic environment (Weston et al., 2009). Fibrates are widely used to treat lipidemic diseases such as hypercholesterolemia and to prevent heart attack (Weston et al., 2009). In the specific case of bezafibrate, maximal concentrations of up to 4.6 and 3.1 $\mu g\ L^{-1}$ have been found in wastewater and surface waters, respectively (Fent et al., 2006; Reis-Santos et al., 2018; Thomas and Hilton, 2004). Yet, most of the available ecotoxicity data for these compounds has been obtained from freshwater organisms (Minguez et al., 2016) with the risk posed by these pharmaceutical compounds to coastal and marine environments and biota still poorly documented. Ecotoxicological assays with bezafibrate have shown immobilization EC50 (half maximal effective concentrations) for *Daphnia magna* ranging from 30.3 to 240.4 mg L^{-1}, while for *Thamnocephalus platyurus* and *Anabaena* sp. EC50 were 39.69 and 7.62 mg L^{-1}, respectively (Han et al., 2006; Isidori et al., 2007; Rosal et al., 2010). Claessens et al. (2013) determined an EC50 dose of bezafibrate for *P. tricornutum* of 0.355 mg L^{-1}. Ultimately, baseline ecotoxicological data on marine organisms is paramount to delineate adequate measures to safeguard marine environments (Marchand and Tissier, 2007; Minguez et al., 2016).

At the base of every marine system are the phototrophs, cycling the energy of the sun, soaking carbon and fueling the trophic web. Any disturbance at this level has inevitable impacts throughout the marine ecosystems. Emerging pollutants are known to impair the photosynthetic metabolism of phototrophic organisms (Anjum et al., 2016; Cabrita et al., 2016; Santos et al., 2014). Although these impacts are well described at sub-cellular level for some contaminants, like metals and metalloids (see Anjum et al., 2016, and references herein), to the best of our knowledge, no photochemical-based ecotoxicity studies have yet been done regarding pharmaceuticals. Remote sensing techniques such as Pulse amplitude modulated (PAM) fluorometry arise as potential non-invasive high-throughput screening (HTS) tools (Cabrita et al., 2017; Santos et al., 2014) to evaluate ecotoxicity in phototrophic organisms. These techniques evaluate the photonic energy harvest and transformation processes into electronic energy, using the involved pigments, their fluorescence and spectral signatures signals as proxy (Anjum et al., 2016; Cabrita et al., 2016; Santos et al., 2014). Any change at the primary productivity level can be efficiently assessed by these techniques (Duarte et al., 2017b; Feijão et al., 2017), and have proved to evaluate contaminants' effects at a physiological level with a dose-related response (Anjum et al., 2016; Cabrita et al., 2017; Santos et al., 2014).

Marine microalgae are promising biomonitor organisms, having simultaneously a high ecological importance as base of marine food webs (Guschina and Harwood, 2009a), and have been shown to act as bioindicator of disturbance under natural conditions and extreme contamination events (Cabrita et al., 2017, 2016, 2014). Specifically, phytoplankton is probably the first compartment to be affected by contaminants. As small (0.2–200 μm) single or chain-forming cells suspended in water, phytoplankton have very high surface-to-volume ratios, respond quickly to suspended toxicants with high uptake rates, and therefore can provide sensitive and effective biomarkers of contaminant stress (Cabrita, 2014; Cabrita et al., 2017, 2016; Gameiro et al., 2016). Additionally phytoplankton are the major marine producers of many complex biomolecules, including fatty acids present in diverse lipid classes (Guschina and Harwood, 2009b). Photosynthetic organisms can synthetize linoleic- and linolenic acids, which belong to omega-6 (ω-6) and omega-3 (ω-3) classes, respectively, and are essential fatty acids (EFA) for vertebrates. EFA are precursors of long chain polyunsaturated fatty acids (LC-PUFAs), such as eicosapentaenoic acid (EPA) and docosahexaenoic acid (DHA), which play key roles in various biological functions, including heart health, immune and inflammatory responses, visual acuity, as well as being major components of neurological tissues (see review from Wiktorowska-Owczarek et al. (2015)). Since most organisms in the higher trophic levels of marine food webs, such as fish and humans, have limited ability to produce LC-PUFA from EFA, they obtain them through diet, relying on their de novo production by aquatic algae (Arts et al., 2001).

Due to their widespread presence in the marine environment, it is paramount to evaluate the effects of pharmaceuticals at the primary productivity level. In the present study, we aim to assess the ecotoxicological effects of bezafibrate exposure, at environmentally relevant concentrations such as the ones found in the vicinity of wastewater outfalls, in the primary productivity and fatty acid composition of a cosmopolitan model diatom *Phaeodactylum tricornutum*, and its potential impact on coastal marine or estuarine ecosystems.

2. Material and methods

2.1. Experimental setup

Monoclonal cultures of model diatom *P. tricornutum* Bohlin (Bacillariophyceae) (IO 108–01, IPMA) were grown in 250 ml of f/2 medium (Guillard and Ryther, 1962) under controlled conditions for 6 days

(18 ± 1 °C, under constant aeration and a 12 h light: 12 h dark photoperiod). A growth chamber was programmed with a sinusoidal function simulating sunrise and sunset, with a light intensity at noon simulating a natural light environment (RGB 1:1:1, Maximum PAR 80 μmol photons m^{-2} s^{-1}, 14/10 h day/night rhythm). Initial cell concentration was approximately 2.7×10^5 cells ml^{-1}, following the Organization for Economic Cooperation and Development (OECD) guidelines for algae bioassays (OECD, 2011) and the therein recommended initial cell density for microalgae cells with similar size to *P. tricornutum*. Cultures were exposed to a bezafibrate concentration gradient (0, 3, 6, 30 and 60 μg L^{-1}) prepared by dissolving aliquots of a bezafibrate stock solution (1 g L^{-1} in 5% DMSO 5%) in the culture flasks (Drechsel-type gas-washing bottles) with growth medium. Exposure occurred 48 h after inoculation and during another 48 h (Cabrita et al., 2017; Feijão et al., 2017). Exposure took place after inoculation to ensure that it was applied during the exponential growth phase (Cabrita et al., 2017; Feijão et al., 2017). Final DMSO concentration in the culture flasks ranged from 0.002 to 0.00003% and controls were performed to dismiss possible carrier solution effects at the final concentration in the culture flasks. No carrier effects were detected under exposure to the tested DMSO concentrations when compared to a control culture (data not shown). According to Kunkel and Radke (2008) bezafibrate under the tested conditions in the present study, has a half-life time of 4.3 days, supporting the duration of 48 h exposure trials at the selected concentrations. For every bezafibrate concentration three replicates were made. All labware used in the experiments was washed with HNO_3 (20%) for two days, rinsed thoroughly with ultra-pure water and autoclaved to avoid contamination. All culture manipulations were performed in a laminar air flow chamber under standard aseptic conditions.

2.2. Growth rates and cell harvesting

Cell counting of *P. tricornutum* samples under different bezafibrate concentrations were performed in a Neubauer improved counting chamber, with an Olympus BX50 (Tokyo, Japan) inverted microscope, at 400-times magnification. Growth resulted from the difference between initial and final logarithmic cell densities divided by the exposure period (Santos-Ballardo et al., 2015), and was expressed as the mean specific growth rate per day. Samples for biochemical analysis were collected after 48 h of exposure to bezafibrate (correspondent to 5 days after inoculation). After centrifugation (4000 ×*g* for 15 min at 4 °C) and supernatant removal, pellets were immediately frozen in liquid nitrogen and stored at −80 °C. Three biological replicates for each analysis were collected from a total of 15 experimental units.

2.3. Chlorophyll a pulse amplitude modulated (PAM) fluorometry

Pulse amplitude modulated (PAM) chlorophyll fluorescence measurements were performed using a FluoroPen FP100 (Photo System Instruments, Czech Republic), on samples using a 1 ml cuvette. Cell density was assessed daily for comparison purposes using a non-actinic light (Ft). All fluorometric analyses were carried out in dark-adapted samples. Analysis of chlorophyll transient light curves were carried using the OJIP test, which can be divided in 4 main steps. Level O (first step) represents all the open reaction centres at the onset of illumination with no reduction of Q_A (fluorescence intensity lasts for 10 ms). The rise of transient from O to J (second step) indicates the net photochemical reduction of Q_A (the stable primary electron acceptor of PSII) to Q_A^- (lasts for 2 ms). The phase from J to I (third step) was due to all reduced states of closed RCs such as Q_A^- Q_B^-, Q_A Q_B^{2-} and Q_A^- Q_BH_2 (lasts for 2–30 ms). The level P (300 ms, fourth step) coincides with maximum concentration of Q_A^- Q_B^2 with plastoquinol pool maximally reduced. The phase P also reflects a balance between light incident at the PSII side and the rate of utilization of the chemical (potential) energy and the rate of heat dissipation (Cabrita et al., 2017; Feijão et al., 2017; Zhu et al., 2005). From this analysis, several photochemical parameters were attained (Table 1).

2.4. Pigment analysis

Pigments were extracted from sample pellets with 100% acetone and maintained in cold ultra-sound bath for 2 min, to ensure complete disaggregation of the cell material. Temperature and time of extraction were −20 °C and 24 h in the dark to prevent degradation (Cabrita et al., 2017, 2016; Feijão et al., 2017). Samples were then centrifuged for 15 min at 4000 ×*g* and at 4 °C. Dual beam spectrophotometer was used to scan supernatants from 350 nm to 750 nm at 0.5 nm steps. The absorbance spectrum was introduced in the Gauss-Peak Spectra (GPS) fitting library, using SigmaPlot Software. Pigment analysis was employed using the algorithm developed by Kupper et al. (2007), enabling the detection of Chlorophyll *a* and *c*, Pheophytin a, β-carotene, Fucoxanthin, Diadinoxanthin (DD) and Diatoxanthin (DT).

2.5. Fatty acid profiles

Fatty acid analysis was performed by direct trans-esterification of cell pellets, in freshly prepared methanol sulfuric acid (97.5:2.5, v/v), at 70 °C for 60 min, as previously described for this diatom (Feijão et al., 2017). Pentadecanoic acid (C15:0) was used as internal standard. Fatty acids methyl esters (FAMEs) were recovered using petroleum ether, dried under a N_2 flow and re-suspended in an appropriate amount of hexane. One microliter of the FAME solution was analysed in a gas chromatograph (Varian 430-GC gas chromatograph) equipped with a hydrogen flame ionization detector set at 300 °C. The temperature of the injector was set to 270 °C, with a split ratio of 50. The fused-silica capillary column (50 m × 0.25 mm; WCOT Fused Silica, CP-Sil 88 for FAME; Varian) was maintained at a constant nitrogen flow of 2.0 ml min^{-1} and the oven set at 190 °C. Fatty acids were identified by comparison of retention times with standards (Sigma-Aldrich) and chromatograms analysed by the peak surface method, using the Galaxy software. The double bond index (DBI), a typical indicator of the membrane saturation levels (Feijão et al., 2017), was calculated as follows:

$$DBI = \frac{2 \times (\%monoenes + 2 \times \%dienes + 3 \times \%trienes + 4\%tetraenes + 5 \times pentaenes)}{100}$$

Table 1
Summary of fluorometric analysis parameters and their description.

OJIP-test	
Area	Corresponds to the oxidized quinone pool size available for reduction and is a function of the area above the Kautsky plot
N	Reaction centre turnover rate
S_M	Corresponds to the energy needed to close all reaction centres
M_0	Net rate of PS II RC closure.
γ_{RC}	Probability that a PSII chl molecule function as a RC
ABS/CS	Absorbed energy flux per cross-section.
TR/CS	Trapped energy flux per cross-section
ET/CS	Electron transport energy flux per cross-section
DI/CS	Dissipated energy flux per cross-section.
RC/CS	Number of available reaction centres per cross section
TR_0/DI_0	The contribution or partial performance due to the light reactions for primary photochemistry
$\delta R_0 / (1 - \delta R_0)$	Contribution of PSI, reducing its end acceptors
$\psi_0 / (1 - \psi_0)$	Contribution of the dark reactions from Q_A^- to PC
$\psi_{E0} / (1 - \psi_{E0})$	Equilibrium constant for the redox reactions between PS II and PS I
RE_0/RC	Electron transport from PQH_2 to the reduction of PS I end electron acceptors
RC/ABS	Reaction centre II density within the antenna chlorophyll bed of PS II

2.6. Statistical analysis

For each variable considered in this study (i.e. growth, photobiological and biochemical variables), differences among bezafibrate treatment levels were evaluated through non-parametric Krustal-Wallis tests, due to aa lack of normality and homogeneity of variances in the data. Spearman correlation tests were applied to assess the relationship between the exogenous dose applied and the photochemical and biochemical variables. In order to evaluate the changes in the whole photochemical metabolism and in the complete fatty acid profile, a multivariate approach was applied (Duarte et al., 2018, 2017b). Multivariate statistical analyses were conducted using Primer 6 software (Clarke and Gorley, 2006), using non-parametric multivariate analysis packages. Data regarding the fatty acid relative composition and the photochemical variables studied, were used to construct two resemblance matrixes based in the Euclidean distances between samples. Canonical Analysis of Principal coordinates (CAP) was used to generate statistical multivariate models based in fatty acid relative composition and relevant photochemical variables, and to classify and separate the different treatment groups. This multivariate approach is insensitive to heterogeneous data and frequently used to compare different sample groups using the intrinsic characteristics of each group (metabolic characteristics) (Cabrita et al., 2017; Duarte et al., 2018, 2017b).

3. Results

3.1. Cell growth rates

Considering the cell density of the *P. tricornutum* cultures exposed to the different levels of bezafibrate, it was possible to observe that the higher concentrations of this substance induced a higher number of cells per unit of volume of culture (Fig. 1). At the basis of this increase in cell density is probably the increasing number of divisions per day and reduced doubling time, resulting in an increasing trend in specific growth rate, although neither of these parameters was statistically significant. Nevertheless, a positive correlation could be observed between the exogenous bezafibrate concentration and the specific growth rate and doubling times ($r^2 > 0.60$).

3.2. Diatom photochemistry

Analyzing the four main energy fluxes that represent the overall photochemical process from light harvesting electronic transport, some distinct evidences could be observed regarding the individuals exposed to the different concentrations of bezafibrate (Fig. 2). No differences were found in the amount of energy absorbed by the PS II antennae (ABS/CS). Nevertheless, the energy flux that was effectively trapped inside the PS II (TR/CS) and transported within the electronic transport chain (ETC) (ET/CS) suffered significant decreases with increasing bezafibrate concentrations. Although not statistically significant, it was also possible to observe a tendency for increasing energy dissipation flux (DI/CS) and for a reduction of the number of oxidized PS II reaction centres (RC/CS).

At the basis of these energy transduction impairments are changes in the functioning of different components of the photosystems and of the ETC (Fig. 3). At the lowest bezafibrate concentrations (3 and 6 $\mu g\ L^{-1}$), the ETC evidenced different patterns. All the parameters related to quinone pool size and functioning suffered a marked increase. Specifically, there was an increase in the oxidized quinone pool size (available for electron transport), an enhancement in the number of Q_A redox turnovers until maximum fluorescence is reached (N), as well as a rise in the energy needs to close (reduce) all RCs (S_M). At the highest bezafibrate exposure concentrations, there was an evident decrease in the probability that a PS II chlorophyll molecule function as a RC (γ_{RC}), along with a reduction in the Q_A reduction rate (M_0). At these elevated concentrations, the remaining variables showed values similar to the ones found in the control treatment.

A closer analysis of the photochemical processes from PS II to PS I revealed a significant reduction of the contribution of both the light (TR_0/DI_0) and dark ($\psi_0 / 1 - \psi_o$) reactions of the photochemical cycle with increasing bezafibrate concentration (Fig. 4). Moreover, there was a significant reduction of the reaction centre density within the PS II antenna chlorophyll bed (RC/ABS). At the PS I level, there was a significant decline of the contribution of this photosystem in reducing its end-acceptors ($\delta R_0 / 1 - \delta R_0$), leading to a shift in the equilibrium constant for the redox reaction between both photosystems towards the PS II ($\psi Eo / (1 - \psi Eo)$). Finally, the lack of PSII activity results from changes to the ETC, and not due to intrinsic changes in the PS I. This is confirmed by the maintenance in the electron transport from PQH_2 to the reduction of the PS I end acceptors (RE_0/RC).

3.3. Diatom pigment composition

Pigment profile of *P. tricornutum* cultures exposed to the different bezafibrate concentrations (Fig. 5) indicated that several pigments were severely affected. Chl *a* and *c*, alongside with fucoxanthin, diadinoxanthin and diatoxanthin showed a significant concentration decrease on a cell basis ($r^2 < -0.70$). This pattern was most evident in

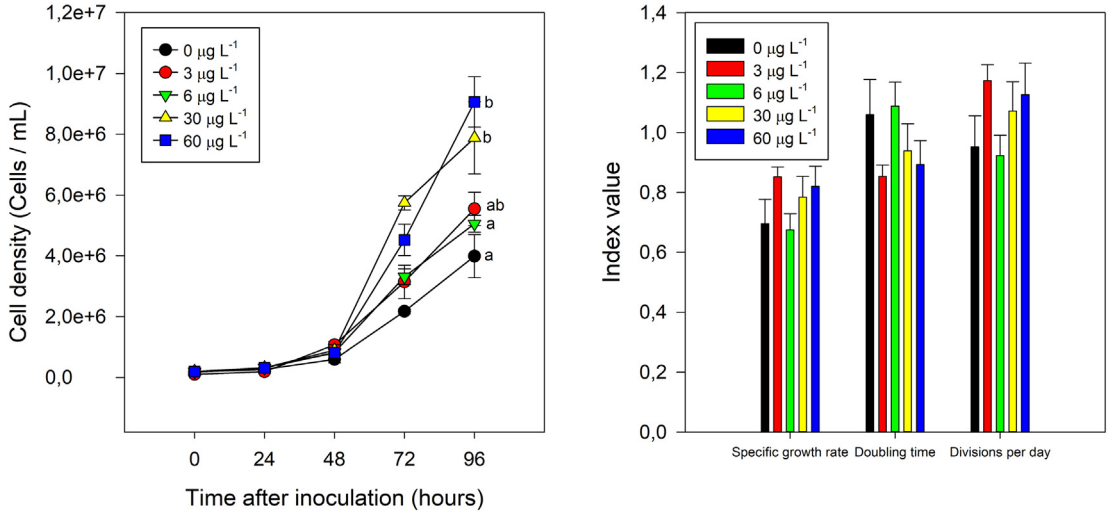

Fig. 1. Cell density and derived growth parameters of *Phaeodactylum tricornutum* following a 48 h exposure to different bezafibrate concentrations (average ± standard deviation, $N = 3$, different letters indicate significant differences at $p < 0.05$).

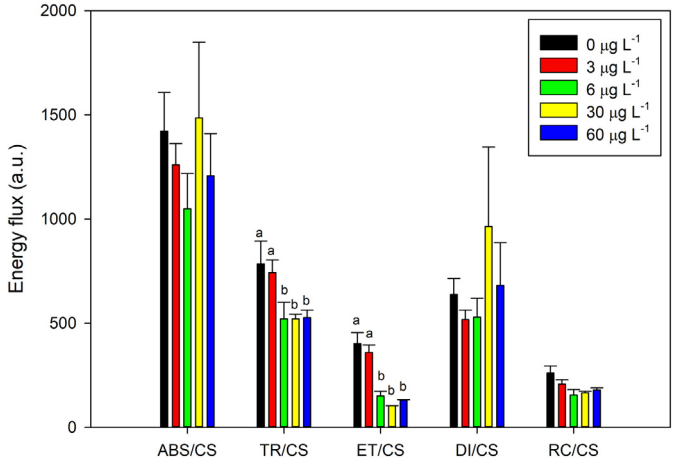

Fig. 2. *Phaeodactylum tricornutum* phenomological energy fluxes (absorbed (ABS/CS, trapped (TR/CS), transported (ET/CS) and dissipated (DI/CS)) and number of available reaction centres per cross section (RC/CS), following a 48 h exposure to different bezafibrate concentrations (average ± standard deviation, N = 3, different letters indicate significant differences at $p < 0.05$).

fucoxanthin, which showed extremely low values under exposure to the highest bezafibrate dose ($r^2 = -0.90$). However, in general only the highest bezafibrate concentration elicited significant effects on pigment concentrations.

3.4. Diatom fatty acid profile

The fatty acid profile of *Phaeodactylum tricornutum* exposed to different bezafibrate concentrations showed no significant differences in individual fatty acid relative concentrations or in the derived ratios, mostly due to the intra-treatment variability (Fig. 6). Nevertheless, some correlations could be established between fatty acid data and the exogenous dose applied. Concentrations of monounsaturated palmitoleic acid (16:1) showed a positive correlation ($r^2 = 0.70$) with exogenous bezafibrate dose. Inversely, the chloroplastidial fatty acids di-unsaturated hexadecadienoic acids (16:2 n-4 and n-7), tri-unsaturated hexadecatrienoic acid (16:3), and hexadecatetraenoic acid (16:4) showed negative correlations (r^2 between −0.70 and −0.60) with increasing bezafibrate concentrations. Despite individual correlations with exposure dose, multivariate patterns were more sensitive to dose-response patterns. A strong negative correlation ($r^2 = -0.70$) between the relative abundance of MUFAs and the external bezafibrate concentration was observed. UFAs relative abundance and the UFA/SFU showed a positive correlation ($r^2 = 0.70$) with the external doses applied.

3.5. Multivariate classification

The multivariate CAP analysis using the photochemical data and the fatty acid profile of diatom samples exposed to different levels of bezafibrate, produced two similar classifications (Fig. 7). The CAP plot based on the photochemical data separated the individuals exposed to intermediate bezafibrate concentration of 6 μg L^{-1}, from control, lower concentration and another group of higher exposure concentrations. The CAP analysis of fatty acid relative abundances produced a similar group classification but the control group was separated while individuals exposed to intermediate (3 and 6 μg L^{-1}) bezafibrate were grouped. Additionally, it was also possible to disentangle samples from the groups exposed to 30 and 60 μg L^{-1} of bezafibrate. Using only the photochemical data this separation was not achieved. Both CAP analysis produced models with elevated classification efficiency (73.3% using the photochemical data and 53.3% using the fatty acid profile).

4. Discussion

Phaeodactylum tricornutum cultures exposed to bezafibrate showed increased cell density. In fact, Claessens et al. (2013) found no growth inhibition effects in *P. tricornutum* at concentrations above the water solubility of bezafibrate (0.355 mg L^{-1}). Notwithstanding, several photochemical related variables seem to indicate a lower photosynthetic efficiency. Although this is an apparent contradiction, we hypothesize that the increased growth observed in *P. tricornutum* exposed to high exogenous bezafibrate concentrations likely resulted from a shift in its metabolism from autotropic to mixotrophic. There are evidences that some diatoms can shift metabolism to a mixotrophic state, wherein both light and external reduced carbon contribute to biomass accumulation (Cerón-García et al., 2013; Cerón García et al., 2005; Semple et al., 1999; Villanova et al., 2017). In the presence of aromatic compounds (as is the case of bezafibrate), other diatom species have been shown to be able to transform and degrade these molecules and utilize the sub-products for mixotrophic growth (Maeng et al., 2018; Semple et al., 1999). The several photochemical features still active in *P. tricornutum* support the hypothesis of a shift to mixotrophy undergone by this species, as diatoms do not change to an heterotrophic state but rather to a mixotrophic state were light is still required (Maeng et al., 2018). Nevertheless, the bezafibrate catabolic pathway inside the cells is not known, and thus specific deeper metabolomic studies are required to confirm this hypothesis. One of the first features regarding this lower photosynthetic efficiency is a reduced ability of the diatoms to trap and use the photonic energy. Two mechanisms appear to be involved in this process. At a first level, bezafibrate exposure reduced the chlorophyll molecules available to act as reaction centre, and thus the number of reaction centres available to trap the incident photons. This may be connected to the decrease in the fucoxanthin pigment. In diatoms, the PSII light-harvesting complexes are formed by the fucoxanthin-chlorophyll protein (FCP) complex, making this carotenoid one of the few with light-harvesting capacity (Mann and Myers, 1968). The reduced ability to trap photonic energy and the number of reaction centres available for reduction is intrinsically connected with lower fucoxanthin contents (Feijão et al., 2017).

Additionally, changes in the FA composition of chloroplast membrane lipids can explain unbalances in photosynthesis, through modifications of the redox potential (Kern and Guskov, 2011). Studies already reported that changes in fatty acid composition of polar lipid can be one of the causes of dimerization of PSII (Kruse et al., 2000). On the other hand, there was also a reduced capacity to use the trapped energy in the electron transport chain (ETC). The most abundant thylakoid lipid In *P. tricornutum* is monogalactosidiacylglycerol (MGDG), generally composed by 16:3 fatty acid (Feijão et al., 2017). The reduction of the chloroplastidial fatty acids 16:2, 16:3 and 16:4 in proportion to increasing bezafibrate dose can be the basis for the cells' reduced ability to use the ETC-generated redox potential. In fact, the concentration of this fatty acid showed a strong inverse correlation with the dose applied ($r^2 = -0.70$). This would lead to a reduced amount of quinones anchored to this membrane system. Moreover, it is also possible to observe that, at the functional level, the quinones present in the ETC are also less efficient, as shown by the lower Q_A reduction rate. Consequentially, strong impacts on the PS I level were observed. Alterations in FAs composition and the influence of increased unsaturation on membrane properties, such as those promoted by bezafibrate exposure, are connected to decreased photosynthetic performance, as highlighted in studies focusing on cation-imposed stress in photosynthetic organisms (Allakhverdiev et al., 2001, 1999; Duarte et al., 2017a). The lack of energy transduction from the PS II to the ETC leads to a potentially lethal situation of excessive redox accumulation within the photosystems, which could lead to photoinhibition and to the destruction of D1 protein, and consequent deactivation of the PS II repair cycle and its irreversible inactivation (Havurinne and Tyystjärvi, 2017). Nevertheless, the enzymatic mechanisms available for energy dissipation (xanthophyll cycle, data not

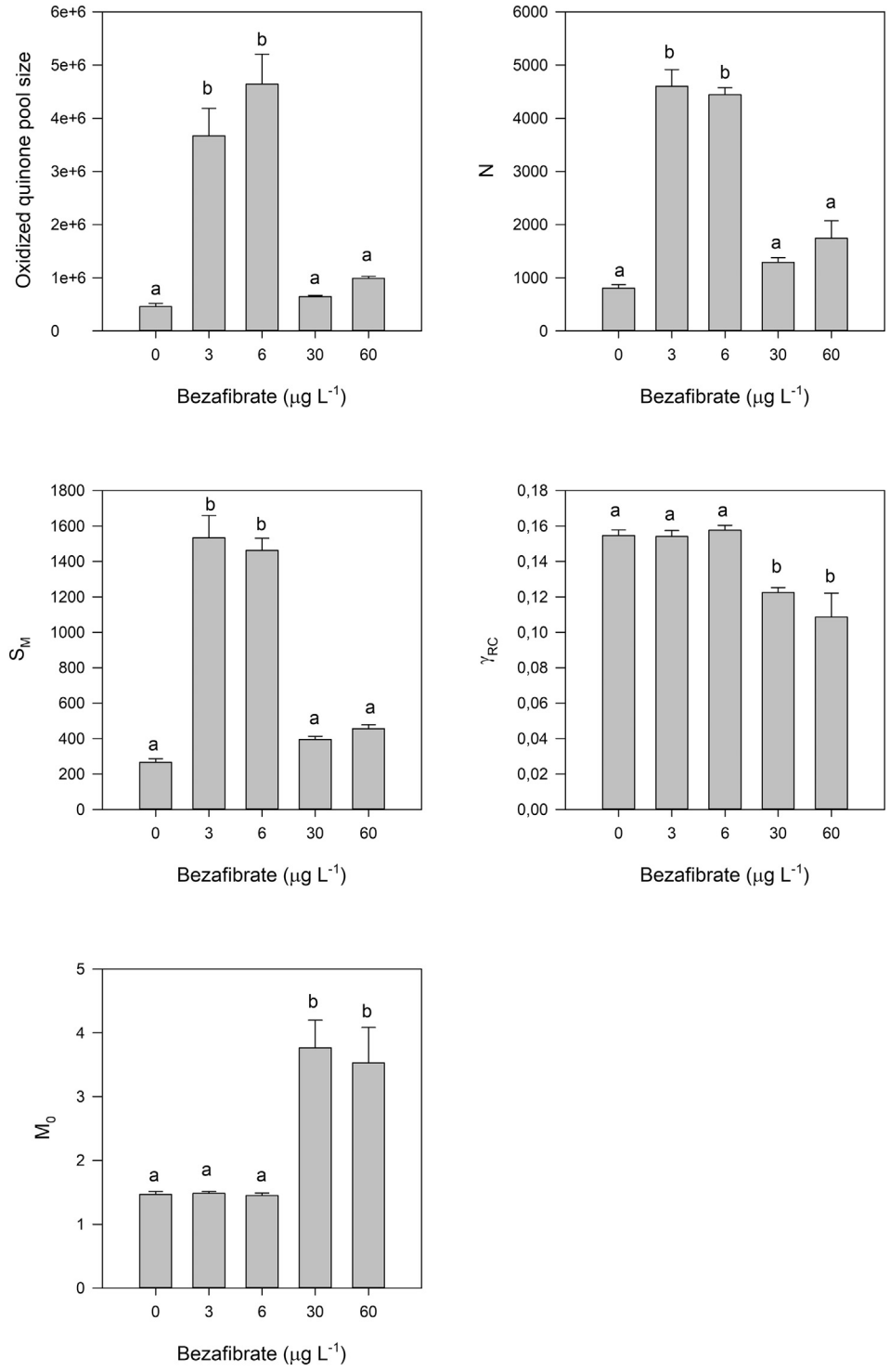

Fig. 3. *Phaeodactylum tricornutum* PS II and ETC related photochemical traits (reaction centre turnover rate (N), energy needed to close all reaction centres (S_M), net rate of PS II RC closure (M_0), probability that a PSII chl molecule function as a RC (γ_{RC}) and oxidized quinone pool), following a 48 h exposure to different bezafibrate concentrations (average ± standard deviation, N = 3, different letters indicate significant differences at $p < 0.05$).

shown) were not activated. The absence of significant differences in the activity of these enzymatic energy dissipation mechanisms between treatments, coupled with high dissipated energy flux under exposure to high bezafibrate, could indicate that the accumulated energy at the PS II donor side is efficiently diverted from the photosystems and consequently the enzymatic photoprotection mechanisms were not activated (Lavaud et al., 2002).

As the energy transduction throughout the ETC was not effectively processed, there were lower amounts of energy reaching the PS I. Nevertheless, the effectiveness of the energy transport from the last ETC quinone (PQH_2) to the PS I was not affected (RE0/RC). As any other effectiveness variable, RE0/RC is based on the energetic yield, and thus is only based on the energy that reaches the PQH_2 and the relative amount that is transported to the PS I. This severely shifts the redox equilibrium between photosystems towards the PS II (ψEo/(1-ψEo)). This lack of redox potential reaching the PS I impairs both the light and dark reactions of photosynthesis, and ultimately the regeneration of energetic substrates at the PS I level (Duarte et al., 2017b).

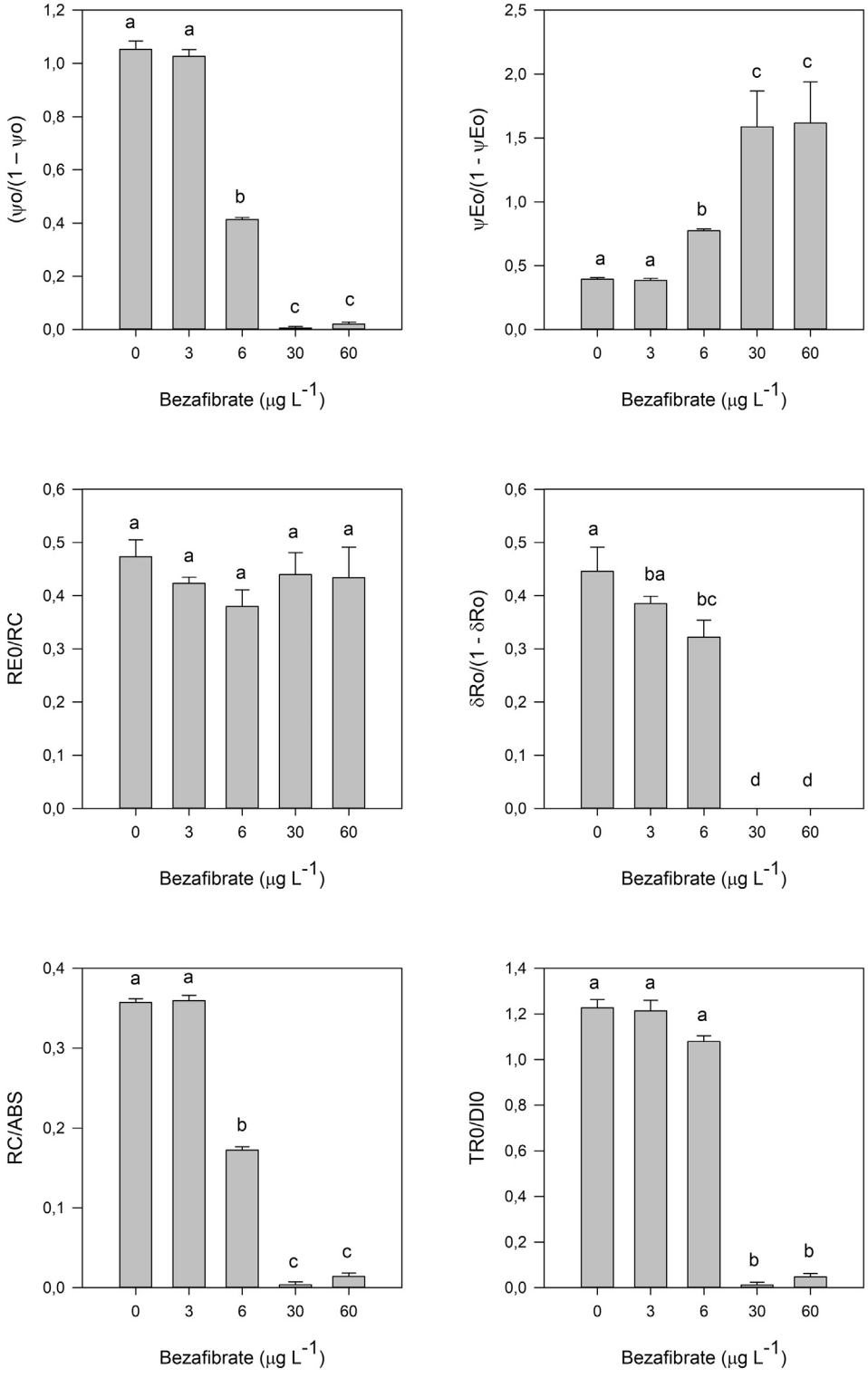

Fig. 4. *Phaeodactylum tricornutum* PS II and PS I photochemical traits (contribution or partial performance due to the light reactions for primary photochemistry (TR_0/DI_0) contribution of PSI, reducing its end acceptors (δR_0), contribution of the dark reactions from quinone A to plastoquinone ($\psi_0 / (1 - \psi_0)$), equilibrium constant for the redox reactions between PS II and PS I ($\psi_{E0} / (1 - \psi_{E0})$), electron transport from PQH_2 to the reduction of PS I end electron acceptors (RE_0/RC) and reaction centre II density within the antenna chlorophyll bed of PS II), following a 48 h exposure to different bezafibrate concentrations (average ± standard deviation, N = 3, different letters indicate significant differences at $p < 0.05$).

Taking in consideration the suggested mixotrophic-shift hypothesis, organisms will use light-generated redox potential to breakdown the carbon substrates acquired from the growing medium (Cerón García et al., 2005; Maeng et al., 2018; Semple et al., 1999). As the trapped energy is not reaching the ETC nor the PS I, this may indicate that this redox potential is being diverted to breakdown aromatic bezafibrate, providing a carbon source for primary metabolism, and thus explaining the increased number of cells with increasing bezafibrate dose. As a lipid-lowering drug, significant effects of exposure on fatty acid profile levels were anticipated. However, differences found were small and only detected through a multivariate analysis. The mixotrophic shift hypothesis here proposed, provides an additional defence mechanism to

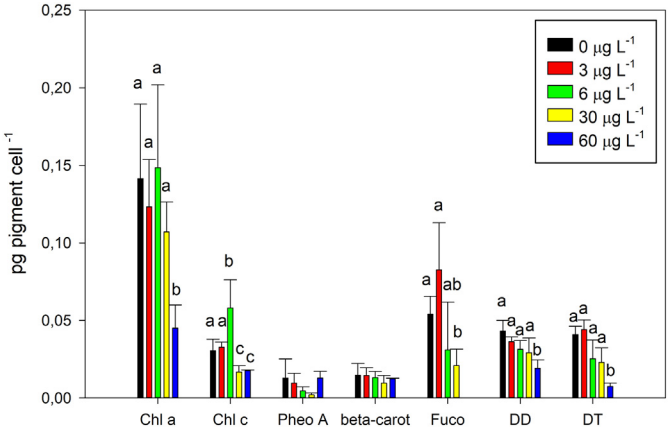

Fig. 5. *Phaeodactylum tricornutum* pigment profile following a 48 h exposure to different bezafibrate concentrations (average ± standard deviation, N = 3, different letters indicate significant differences at $p < 0.05$). Pigments include chlorophyll *a* (Chl *a*), chlorophyll *c* (Chl *c*), pheophytin *a* (Pheo *a*), β carotene (beta-carot), fucoxanthin (Fuco), diadinoxanthin (DD) and diatoxanthin (DT) content.

P. tricornutum, protecting their lipidome from the potential degradation of cell storage lipids triacylglycerols (TAG), following bezafibrate exposure. TAG in diatoms is mostly composed by 16:0 fatty acids (Li et al., 2014), thus an effect of bezafibrate on this lipid compartment would have resulted in a decrease in this fatty acid content, which was not observed. In fact, there was a tendency for enhanced 16:0 cell content with increasing bezafibrate doses, again reinforcing the occurrence of a possible mixotrophic shift, where bezafibrate is being metabolized and thus its effect is not felt as lipid-lowering drug decreasing TAG content. From a biotechnological perspective, *P. tricornutum* may be a candidate diatom – for environmental management, pollution control, biotechnology, environmental remediation, waste water treatment – due to its ability to use or transform bezafibrate. The effects imposed by bezafibrate exposure differ greatly from the ones verified in animals. In *P. tricornutum* there is no effect at the storage lipids level (16:0), as bezafibrate does not act in storage lipids present in liposomes (principal storage compartment in plants and in this diatom), but in TAG fatty acids circulating in the bloodstream (Pahan, 2006). Nevertheless, further assessments on metabolites and water toxicity are required as well as future targeted studies to evaluate the use of bezafibrate as a carbon source in *P. tricornutum* and the environmental threshold and conditions when this occurs.

The application of two CAP analyses proved to be the more efficient in assessing the effects of bezafibrate on the *P. tricornutum* bioenergetic and lipid metabolism. The induction of a metabolic shift, towards a possible mixotrophic situation, at concentrations above 30 µg L^{-1} supports an inability of the photochemical traits to describe and classify the samples according to the differences observed at the photochemical apparatus. However, at moderate concentrations, the photochemical processes showed significant changes in the multivariate analysis that allowed the

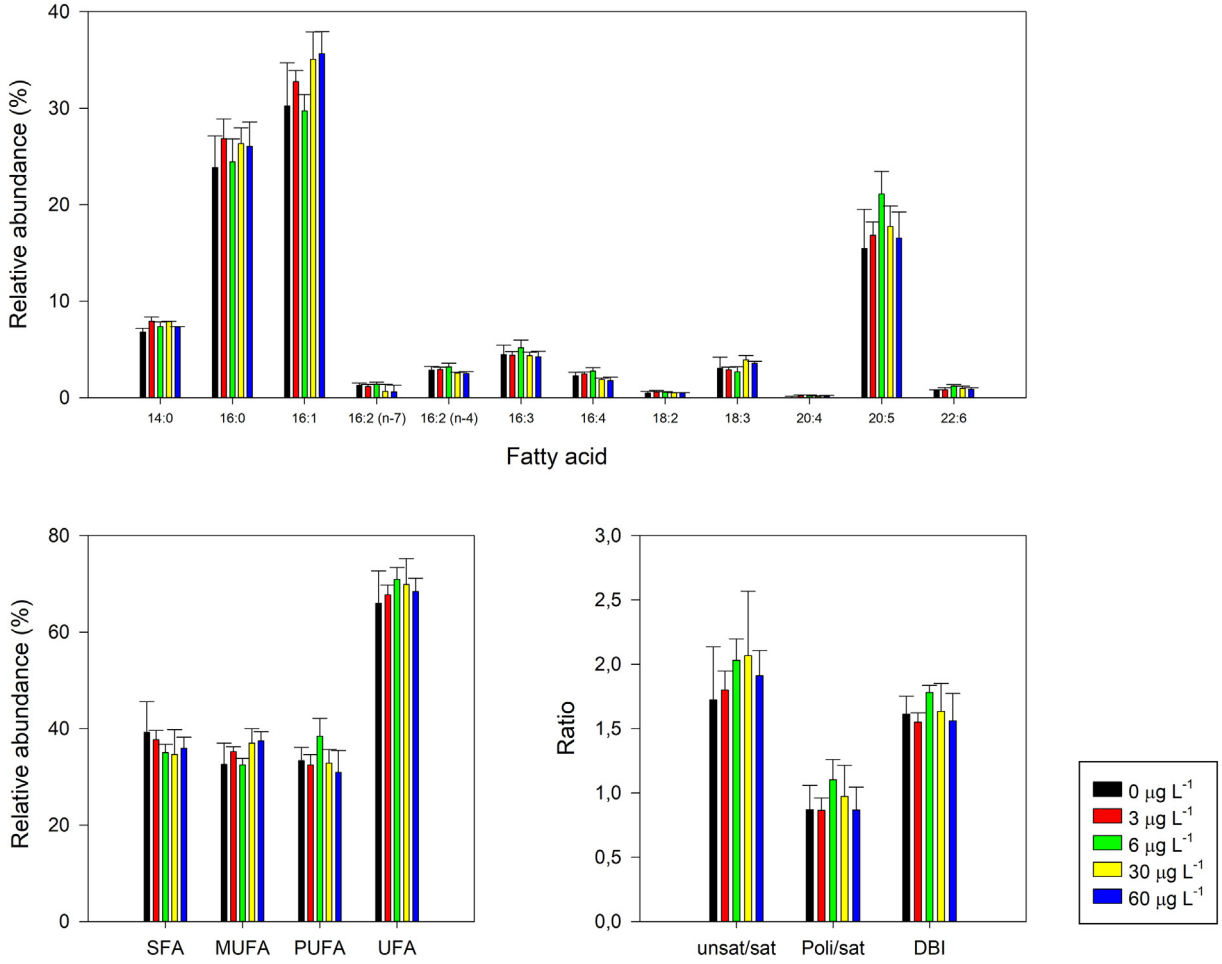

Fig. 6. Fatty acid profile of *Phaeodactylum tricornutum*, following exposure to different concentrations of bezafibrate. Individual fatty acids (FA), major FA classes (saturated fatty acids (SFA), monounsaturated fatty acids (MUFA), polyunsaturated fatty acids (PUFA) and unsaturated fatty acids (UFA) relative abundance) and FA ratios (unsaturated to saturated fatty acids ratio (unsat/sat), polyunsaturated to saturated fatty acids ratio (poly/sat) and double bound index (DBI)) are presented (average ± standard deviation, N = 3, different letters indicate significant differences at $p < 0.05$).

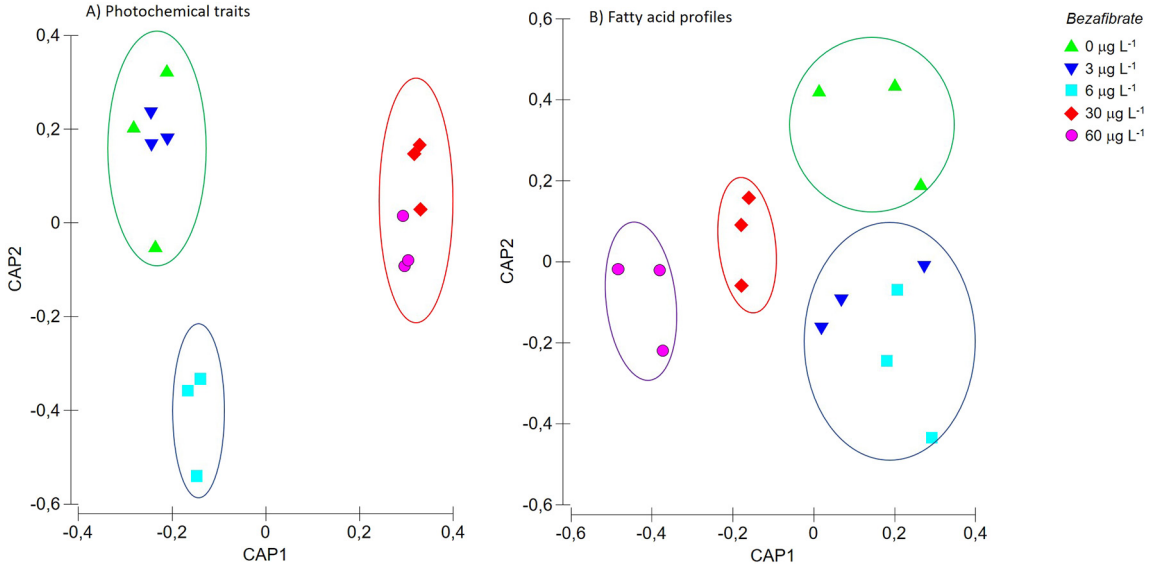

Fig. 7. Canonical analysis plot based on photochemical traits (A) and fatty acid profile (B) of *Phaeodactylum tricornutum* exposed to different bezafibrate concentrations for 48 h. Ellipses group samples with lower statistical distance.

identification of the different bezafibrate exposure treatments. Applying the same canonical approach using the fatty acids profile as basis, the cells undergoing the proposed mixotrophic-state (>30 μg L^{-1} exogenous bezafibrate) are efficiently separated and classified into two distinct groups. As in previous studies (Cabrita et al., 2017; Duarte et al., 2018, 2017b), multivariate analysis proved to be a more efficient approach for classifying distinct exposure groups (diatom samples exposed to bezafibrate), where univariate analysis could not detect variations (e.g. at the fatty acid level).

5. Conclusion

From an ecotoxicological point of view it is clear from this study that bezafibrate affects marine diatoms, especially at high concentrations. Moreover, some photochemical and biochemical traits presented a clear dose-response behavior and therefore can be used as potential biomarkers of exposure. Cell density changes were found not to reproduce the traditional toxic effect of contaminants usually lowering microalgal biomass. Instead, combined changes in the growth and photosynthetic features, indicate a possible bezafibrate induction of mixotrophy in *P. tricornutum*, which highlights the potential repercussions to heterotrophic organisms that rely on diatoms O_2 production and CO_2 harvesting. According to this mixotrophic-hypothesis, *P. tricornutum* can use bezafibrate as carbon source increasing its biomass without producing the essential oxygen upon which marine fishes and invertebrates depend.

Acknowledgements

The authors would like to thank Fundação para a Ciência e a Tecnologia (FCT) for funding the research via project grants PTDC/MAR-EST/3048/2014 (BIOPHARMA), PTDC/CTA-AMB/30056/2017 (OPTOX), UID/MAR/04292/2013 and UID/MULTI/04046/2013. B. Duarte and P. Reis-Santos were also supported by FCT through post-doctoral grants (SFRH/BPD/115162/2016 and SFRH/BPD/95784/2013, respectively).

References

Allakhverdiev, S.I., Nishiyama, Y., Suzuki, I., Tasaka, Y., Murata, N., 1999. Genetic engineering of the unsaturation of fatty acids in membrane lipids alters the tolerance of synechocystis to salt stress. Proc. Natl. Acad. Sci. U. S. A. 96, 5862–5867. https://doi.org/10.1073/pnas.96.10.5862.

Allakhverdiev, S.I., Kinoshita, M., Inaba, M., Suzuki, I., Murata, N., 2001. Unsaturated fatty acids in membrane lipids protect the photosynthetic machinery against salt-induced damage in *Synechococcus*. Plant Physiol. 125, 1842–1853. https://doi.org/10.1104/pp.125.4.1842.

Anjum, N.A., Duarte, B., Caçador, I., Sleimi, N., Duarte, A.C., Pereira, E., 2016. Biophysical and biochemical markers of metal/metalloid-impacts in salt marsh halophytes and their implications. Front. Environ. Sci. 4, 1–13. https://doi.org/10.3389/fenvs.2016.00024.

Arts, M.T., Ackman, R.G., Holub, B.J., 2001. "Essential fatty acids" in aquatic ecosystems: a crucial link between diet and human health and evolution. Can. J. Fish. Aquat. Sci. 58, 122–137. https://doi.org/10.1139/cjfas-58-1-122.

Cabrita, M.T., 2014. Phytoplankton community indicators of changes associated with dredging in the Tagus estuary (Portugal). Environ. Pollut. 191, 17–24. https://doi.org/10.1016/j.envpol.2014.04.001.

Cabrita, M.T., Raimundo, J., Pereira, P., Vale, C., 2014. Immobilised Phaeodactylum tricornutum as biomonitor of trace element availability in the water column during dredging. Environ. Sci. Pollut. Res. 21, 3572–3581. https://doi.org/10.1007/s11356-013-2362-x.

Cabrita, M.T., Gameiro, C., Utkin, A.B., Duarte, B., Caçador, I., Cartaxana, P., 2016. Photosynthetic pigment laser-induced fluorescence indicators for the detection of changes associated with trace element stress in the diatom model species Phaeodactylum tricornutum. Environ. Monit. Assess. 188. https://doi.org/10.1007/s10661-016-5293-4.

Cabrita, M.T., Duarte, B., Gameiro, C., Godinho, R.M., Caçador, I., 2017. Photochemical features and trace element substituted chlorophylls as early detection biomarkers of metal exposure in the model diatom *Phaeodactylum tricornutum*. Ecol. Indic. 0–1. https://doi.org/10.1016/j.ecolind.2017.07.057.

CAS, 2011. Chemical Abstracts Registry News Release 24 May 2011 "CAS REGISTRY Keeps Pace with Rapid Growth of Chemical Research, Registers 60 Millionth Substance". http://www.cas.org/newsevents/releases/60millionth052011.html.

Cerón García, M.C., Sánchez Mirón, A., Fernández Sevilla, J.M., Molina Grima, E., García Camacho, F., 2005. Mixotrophic growth of the microalga *Phaeodactylum tricornutum*: influence of different nitrogen and organic carbon sources on productivity and biomass composition. Process Biochem. 40, 297–305. https://doi.org/10.1016/j.procbio.2004.01.016.

Cerón-García, M.C., Fernández-Sevilla, J.M., Sánchez-Mirón, A., García-Camacho, F., Contreras-Gómez, A., Molina-Grima, E., 2013. Mixotrophic growth of Phaeodactylum tricornutum on fructose and glycerol in fed-batch and semi-continuous modes. Bioresour. Technol. 147, 569–576. https://doi.org/10.1016/j.biortech.2013.08.092.

Claessens, M., Vanhaecke, L., Wille, K., Janssen, C.R., 2013. Emerging contaminants in Belgian marine waters: single toxicant and mixture risks of pharmaceuticals. Mar. Pollut. Bull. 71, 41–50. https://doi.org/10.1016/j.marpolbul.2013.03.039.

Clarke, K.R., Gorley, R.N., 2006. PRIMER v6: User Manual/Tutorial. Prim. Plymouth UK. https://doi.org/10.1111/j.1442-9993.1993.tb00438.x (192 p.).

Duarte, B., Cabrita, M.T.T., Gameiro, C., Matos, A.R.R., Godinho, R., Marques, J.C.C., Caçador, I., 2017a. Disentangling the photochemical salinity tolerance in *Aster tripolium* L.: connecting biophysical traits with changes in fatty acid composition. Plant Biol. 19, 239–248. https://doi.org/10.1111/plb.12517.

Duarte, B., Pedro, S., Marques, J.C., Adão, H., Caçador, I., 2017b. Zostera noltii development probing using chlorophyll a transient analysis (JIP-test) under field conditions: integrating physiological insights into a photochemical stress index. Ecol. Indic. 76. https://doi.org/10.1016/j.ecolind.2017.01.023.

Duarte, B., Carreiras, J., Pérez-Romero, J.A., Mateos-Naranjo, E., Redondo-Gómez, S., Matos, A.R., Marques, J.C., Caçador, I., 2018. Halophyte fatty acids as biomarkers of anthropogenic-driven contamination in Mediterranean marshes: sentinel species survey and development of an integrated biomarker response (IBR) index. Ecol. Indic. 87. https://doi.org/10.1016/j.ecolind.2017.12.050.

EUROSTAT, 2017. http://epp.eurostat.ec.europa.eu/tgm/table.do?tab=table&init=1&plugin=1&language=en&pcode=ten00011.
Feijão, E., Gameiro, C., Franzitta, M., Duarte, B., Caçador, I., Cabrita, M.T., Matos, A.R., 2017. Heat wave impacts on the model diatom *Phaeodactylum tricornutum*: searching for photochemical and fatty acid biomarkers of thermal stress. Ecol. Indic. https://doi.org/10.1016/j.ecolind.2017.07.058.
Fent, K., Weston, A.A., Caminada, D., 2006. Ecotoxicology of human pharmaceuticals. Aquat. Toxicol. 76, 122–159. https://doi.org/10.1016/j.aquatox.2005.09.009.
Gameiro, C., Utkin, A.B., Cartaxana, P., da Silva, J.M., Matos, A.R., 2016. The use of laser induced chlorophyll fluorescence (LIF) as a fast and non-destructive method to investigate water deficit in Arabidopsis. Agric. Water Manag. 164, 127–136. https://doi.org/10.1016/j.agwat.2015.09.008.
Gavrilescu, M., Demnerová, K., Aamand, J., Agathos, S., Fava, F., 2015. Emerging pollutants in the environment: present and future challenges in biomonitoring, ecological risks and bioremediation. New Biotechnol. 32, 147–156. https://doi.org/10.1016/j.nbt.2014.01.001.
Gaw, S., Thomas, K.V., Hutchinson, T.H., 2014. Sources, impacts and trends of pharmaceuticals in the marine and coastal environment. Philos. Trans. R. Soc. B Biol. Sci. 369, 20130572. https://doi.org/10.1098/rstb.2013.0572.
Guillard, R.R.L., Ryther, J.H., 1962. Studies of marine planktonic diatoms: I. *Cyclotella nana* Hustedt, and *Detonula confervacea* (Cleve) gran. Can. J. Microbiol. 8, 229–239. https://doi.org/10.1139/m62-029.
Guschina, I.A., Harwood, J.L., 2009a. Algal Lipids and Effect of the Environment on Their Biochemistry. In: Kainz, M., Brett, M.T., Arts, M.T. (Eds.), Lipids in Aquatic Ecosystems. Springer New York, New York, NY, pp. 1–24 https://doi.org/10.1007/978-0-387-89366-2_1.
Guschina, I.A., Harwood, J.L., 2009b. Algal lipids and effect of the environment on their biochemistry. In: Kainz, M., Brett, M.T., Arts, M.T. (Eds.), Lipids in Aquatic Ecosystems. Springer New York, New York, NY, pp. 1–24 https://doi.org/10.1007/978-0-387-89366-2_1.
Han, G.H., Hur, H.G., Kim, S.D., 2006. Ecotoxicological risk of pharmaceuticals from wastewater treatment plants in Korea: occurrence and toxicity to *Daphnia magna*. Environ. Toxicol. Chem. 25, 265–271. https://doi.org/10.1897/05-193R.1.
Havurinne, V., Tyystjärvi, E., 2017. Action spectrum of photoinhibition in the diatom *Phaeodactylum tricornutum*. Plant Cell Physiol. 58, 2217–2225. https://doi.org/10.1093/pcp/pcx156.
Isidori, M., Nardelli, A., Pascarella, L., Rubino, M., Parrella, A., 2007. Toxic and genotoxic impact of fibrates and their photoproducts on non-target organisms. Environ. Int. 33, 635–641. https://doi.org/10.1016/j.envint.2007.01.006.
Kern, J., Guskov, A., 2011. Lipids in photosystem II: multifunctional cofactors. J. Photochem. Photobiol. B Biol. 104, 19–34. https://doi.org/10.1016/j.jphotobiol.2011.02.025.
Kruse, O., Hankamer, B., Konczak, C., Gerle, C., Morris, E., Radunz, A., Schmid, G.H., Barber, J., 2000. Phosphatidylglycerol is involved in the dimerization of photosystem II. J. Biol. Chem. 275, 6509–6514. https://doi.org/10.1074/jbc.275.9.6509.
Kunkel, U., Radke, M., 2008. Biodegradation of Acidic Pharmaceuticals in Bed Sediments: Insight From a Laboratory Experiment Biodegradation of Acidic Pharmaceuticals in Bed Sediments: Insight From a Laboratory Experiment. 42, pp. 7273–7279. https://doi.org/10.1021/es801562j.
Kupper, H., Seibert, S., Aravind, P., 2007. A fast, sensitive and inexpensive alternative to analytical pigment HPLC: quantification of chlorophylls and carotenoids in crude extracts by fitting with Gauss-peak-spectra. Anal. Chem. 79, 7611–7627.
Lavaud, J., van Gorkom, H., Etienne, A.-L., 2002. Photosystem II electron transfer cycle and chlorespiration in planktonic diatoms. Photosynth. Res. 74, 51–59. https://doi.org/10.1023/A:1020890625141.
Li, Y.-F., Gao, Y., Chai, Z., Chen, C., 2014. Nanometallomics: an emerging field studying the biological effects of metal-related nanomaterials. Metallomics 6, 220. https://doi.org/10.1039/c3mt00316g.
Maeng, S.K., You, S.H., Nam, J.Y., Ryu, H., Timmes, T.C., Kim, H.C., 2018. The growth of Scenedesmus quadricauda in RO concentrate and the impacts on refractory organic matter, *Escherichia coli*, and trace organic compounds. Water Res. 134, 292–300. https://doi.org/10.1016/j.watres.2018.01.029.
Mann, J.E., Myers, J., 1968. Photosynthetic enhancement in the diatom *Phaeodactylum tricornutum*. Plant Physiol. 43, 1991–1995. https://doi.org/10.1104/pp.43.12.1991.
Marchand, M., Tissier, C., 2007. L'analyse du risque chimique en milieu marin: L'approche méthodologique européenne. Environnement, Risques et Sante 6, 127–141. https://doi.org/10.1684/ers.2007.0037.
Minguez, L., Pedelucq, J., Farcy, E., Ballandonne, C., Budzinski, H., Halm-Lemeille, M.P., 2016. Toxicities of 48 pharmaceuticals and their freshwater and marine environmental assessment in northwestern France. Environ. Sci. Pollut. Res. 23, 4992–5001. https://doi.org/10.1007/s11356-014-3662-5.
OECD, 2011. OECD guidelines for the testing of chemicals. Freshwater alga and cyanobacteria, growth inhibition test. Organ. Econ. Coop. Dev., 1–25 https://doi.org/10.1787/9789264203785-en.
Pahan, K., 2006. Lipid-lowering drugs. Cell. Mol. Life Sci. 63, 1165–1178. https://doi.org/10.1007/s00018-005-5406-7.
Reis-Santos, P., Pais, M., Duarte, B., Caçador, I., Freitas, A., Vila Pouca, A.S., Barbosa, J., Leston, S., Rosa, J., Ramos, F., Cabral, H.N., Gillanders, B.M., Fonseca, V.F., 2018. Screening of human and veterinary pharmaceuticals in estuarine waters: a baseline assessment for the Tejo estuary. Mar. Pollut. Bull. 135, 1079–1084. https://doi.org/10.1016/j.marpolbul.2018.08.036.
Rosal, R., Rodea-Palomares, I., Boltes, K., Fernández-Piñas, F., Leganés, F., Gonzalo, S., Petre, A., 2010. Ecotoxicity assessment of lipid regulators in water and biologically treated wastewater using three aquatic organisms. Environ. Sci. Pollut. Res. 17, 135–144. https://doi.org/10.1007/s11356-009-0137-1.
Santos, D., Duarte, B., Caçador, I., 2014. Unveiling Zn hyperaccumulation in Juncus acutus: implications on the electronic energy fluxes and on oxidative stress with emphasis on non-functional Zn-chlorophylls. J. Photochem. Photobiol. B Biol. 140, 228–239. https://doi.org/10.1016/j.jphotobiol.2014.07.019.
Santos-Ballardo, D.U., Rossi, S., Hernández, V., Gómez, R.V., del Carmen Rendón-Unceta, M., Caro-Corrales, J., Valdez-Ortiz, A., 2015. A simple spectrophotometric method for biomass measurement of important microalgae species in aquaculture. Aquaculture 448, 87–92. https://doi.org/10.1016/j.aquaculture.2015.05.044.
Semple, K.T., Cain, R.B., Schmidt, S., 1999. Biodegradation of aromatic compounds by microalgae. FEMS Microbiol. Lett. 170, 291–300. https://doi.org/10.1016/S0378-1097(98)00544-8.
Thomaidis, N.S., Asimakopoulos, A.G., Bletsou, A.A., 2012. Emerging contaminants: a tutorial mini-review. Glob. Nest J. 14, 72–79.
Thomas, K.V., Hilton, M.J., 2004. The occurrence of selected human pharmaceutical compounds in UK estuaries. Mar. Pollut. Bull. 49, 436–444. https://doi.org/10.1016/j.marpolbul.2004.02.028.
Villanova, V., Fortunato, A.E., Singh, D., Bo, D.D., Conte, M., Obata, T., Jouhet, J., Fernie, A.R., Marechal, E., Falciatore, A., Pagliardini, J., Le Monnier, A., Poolman, M., Curien, G., Petroutsos, D., Finazzi, G., 2017. Investigating mixotrophic metabolism in the model diatom *Phaeodactylum tricornutum*. Philos. Trans. R. Soc. B 372, 20160404. https://doi.org/10.1098/rstb.2016.0404.
Weston, A., Caminada, D., Galicia, H., Fent, K., 2009. Effects of lipid-lowering pharmaceuticals bezafibrate and clofibric acid on lipid metabolism in fathead minnow (*Pimephales promelas*). Environ. Toxicol. Chem. 28, 2648–2655. https://doi.org/10.1897/09-087.1.
Wiktorowska-Owczarek, A., Berezińska, M., Nowak, J., 2015. PUFAs: structures, metabolism and functions. Adv. Clin. Exp. Med. 24, 931–941. https://doi.org/10.17219/acem/31243.
Zhu, X.G., Baker, N.R., Ort, D.R., Long, S.P., DeSturler, E., 2005. Chlorophyll a fluorescence induction kinetics in leaves predicted from a model describing each discrete step of excitation energy and electron transfer associated with Photosystem II. Planta 223, 114–133. https://doi.org/10.1007/s00425-005-0064-4.